

**ELECTRO-CATALYTIC AND PHOTO-
ELECTROCHEMICAL WATER SPLITTING BY
GRAPHITIC CARBON NITRIDE-BASED NANO-
HETEROSTRUCTURES**

PREETI CHAUDHARY



**DEPARTMENT OF CHEMISTRY
INDIAN INSTITUTE OF TECHNOLOGY
OCTOBER 2021**

©Indian Institute of Technology Delhi (IITD), New Delhi, 2021

**ELECTRO-CATALYTIC AND PHOTO-
ELECTROCHEMICAL WATER SPLITTING BY
GRAPHITIC CARBON NITRIDE-BASED NANO-
HETEROSTRUCTURES**

By

PREETI CHAUDHARY

DEPARTMENT OF CHEMISTRY

Submitted

*In fulfilment of the requirements of the degree of Doctor of Philosophy
to the*



**INDIAN INSTITUTE OF TECHNOLOGY
OCTOBER 2021**

Dedicated to my Parents and Teachers

CERTIFICATE

This is to certify that the thesis entitled, “**Electro-catalytic and Photo-electrochemical Water Splitting by Graphitic Carbon Nitride-based Nano heterostructures**” being submitted by Ms. Preeti Chaudhary to the Indian Institute of Technology, Delhi for the award of the degree of **Doctor of Philosophy** in chemistry, is a record of bonafide research work carried out by her. Ms. Preeti Chaudhary has worked under my supervision and guidance, and has fulfilled the requirements for the submission of the thesis, which to our knowledge has reached the requisite standard.

The results contained in this dissertation have not been submitted in part or full, to any other institute for award of any degree or diploma.

Dr. Pravin P. Ingole

Associate Professor

Department of Chemistry

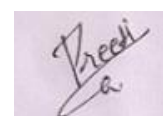
Indian Institute of Technology Delhi

ACKNOWLEDGMENTS

My doctoral dissertation and the research work during my Ph.D would not have been possible without the help and support my supervisor Dr. Pravin P. Ingole . First and foremost, I would like to express my gratitude to my supervisor, for giving me the opportunity to work in this ever evolving and highly demanding field of energy. I also thank for his patience, guidance, constant support and suggestion throughout this journey. I am also motivated to see his enthusiasm towards science and even inspired to see his sincerity, dedication and punctuality even after achieving so much in life. He is an incredible mentor, always encouraging to work hard and move forward. It was his gigantic knowledge of the subject that helped me in understanding various aspects of electrochemistry area. I am whole heartedly thankful for his care and cooperation during stages of my work. I would also like to thank my research committee members; Prof. Sameer Sapra, Prof. Siddharth Pandey and Prof. Rajendra Dhaka for their valuable suggestion to improve my research work. I would like to owe my special thanks to Prof. Sameer Sapra giving me access to use the DRS facility and my senior Dr. Md. Samim Hassan (for fruitful discussions and all time giving helping hand). I am grateful to the Head, Prof Anil. J. Elias, for providing necessary facilities in the department, and all other faculty members and staff and non-teaching staff for their help and assistance during my Ph.D programme.

I am always grateful to the boundless care, support and love of my parents, brother and husband. They always with stand with me to fulfil my dreams and for uplifting of my career.

I bow down the almighty God for blessing me with the health, supporting people and this opportunity in my life.



Preeti Chaudhary

ABSTRACT

The recent challenge for our society is to tackle the present energy crises by moving towards the clean environment and availability of sufficient energy. Interestingly, among the various sources of renewable energy such as solar, biomass, biofuel, geothermal, wind, tidal, solar energy has gained a lot of attention as it is the largest and one of the most promising source for sustainable development without having any compromise with the quality of environment. The generation of hydrogen and oxygen through electrochemical water splitting especially the light assisted i.e. photo-electrochemical (PEC) water splitting reaction is an attractive solution towards sustainable and clean sources of energy. Eventually, it has become one of the prime technologies to answer the sporadic storage problem related to solar energy. The thesis is aimed to synthesize and characterize various nano and nanoheterostructured materials by simple methods such as in-situ heating and hydrothermal for application in photoelectrochemical (PEC) water splitting and hydrogen evolution reaction catalyst. These two areas have immense potential to meet the future energy demands and solve the present energy crises scenario. Transition metal based catalysts are studied due to their many advantages over other metals, such as cost effective features, easy modification of electronic structure, easy synthesis, versatile activity and stability under broad range of pH value.

The thesis deals with the metal oxide nanostructure and nanoheterostructure of metal oxide and graphitic carbon nitride (g-C₃N₄). Photoelectrocatalytic activity for Oxygen evolution reaction and Electro catalytic for Hydrogen evolution reaction were investigated. Synthesis of 2D/2D interfaces between nickel/nickel oxide (Ni/NiO) hexagonal nanosheets with graphitic-carbon nitride (g-C₃N₄) using an in-situ solid-state heat treatment was done, which results in higher electrochemical and PEC water splitting activity of 2D/2D interface depicting a maximum OER photocurrent

density of 20 mA cm^{-2} at an over potential of 190 mV. Varying the ratio of precursors effect for NiO to that of g-C₃N₄ viz. 1:1, 1:8, and 1:16 was also studied. Among which, the highest ratio of NiO to g-C₃N₄ nanosheets (i.e. 1:1) was noted to demonstrate the best performance towards electrochemical (HER) hydrogen evolution reaction showing dramatically reduced over potential to 26 mV to drive a current density of 10 mA cm^{-2} and 1:8 for OER. The enhanced results may be due to the more intimate contact between 2D sheets of NiO with g-C₃N₄. Next Nickel Incorporated Graphitic Carbon Nitride Supported Copper Sulfide reported for Efficient Noble-Metal-Free Photo-electrochemical Water Splitting. These copper sulfides supported on nickel-incorporated graphitic carbon nitride (Ni/g-C₃N₄@CuS) sheets improved the PEC activity due to the formation of p-n junction. The Ni/g-C₃N₄@CuS nanohybrids depicts almost three-fold enhancement in current density under light illumination reaching to 15.5 mA cm^{-2} at an over potential of ca. 600 mV than in the dark and almost fifteen-fold enhancement as compared to its parent materials, CuS and g-C₃N₄. Further work is done on the in-Situ solid-state synthesis combination of hexagonal sheets and tubes a composite of MoO₃/g-C₃N₄ for enhanced photo-electrochemical water splitting. The effect of the composition of g-C₃N₄ sheets to MoO₃ viz. 1:1, 8:1, and 16:1 has been studied. Among these, the 8:1 (i.e. 8 parts g-C₃N₄ and 1 part MoO₃) have been found to be the best for the PEC activity. The said heterojunction leads to improvement in PEC activity by having the photocurrent density of 4.96 mA cm^{-2} at an over potential of 190 mV. Next we tried to study the ternary nanoheterostructures composed of two metal oxides Ni/NiO and Co₃O₄ with graphitic carbon nitride forming 2D/3D interfaces. This formation of ternary nanoheterostrutures leads to the enhanced PEC response, g-C₃N₄/NiNiO/Co₃O₄ was noted to be 2.5 times g-C₃N₄/NiNiO and 5.8 times g-C₃N₄/Co₃O₄ higher than the individual composites. Besides, doing the study on heterojunctions for HER and OER we also tried to develop a catalyst for the study of methanol

oxidation and methanol assisted electrochemical water splitting. We tried to decorate the Ag nanoparticles on the surface of dendritic hematite. We observed the enhanced electro catalytic activity for water splitting with the increase in the addition methanol amount which could be attributed to the synergistic effect of hematite dendrites, larger surface area of dendrite structure leading to higher loading of Ag NPs. Following the chapters in details, the thesis present conclusion and future scope where we plan to modify the g-C₃N₄ by making heterostructures with metal oxide and suggesting new materials to have efficient PEC results and optimizing the charge-transfer process at the interface.

सार

हमारे समाज के लिए हाल की चुनौती स्वच्छ पर्यावरण और पर्याप्त ऊर्जा की उपलब्धता की ओर बढ़ते हुए वर्तमान ऊर्जा संकट से निपटने की है। दिलचस्प बात यह है कि अक्षय ऊर्जा के विभिन्न स्रोतों जैसे सौर, बायोमास, जैव ईंधन, भूतापीय, पवन, ज्वार, सौर ऊर्जा ने बहुत ध्यान आकर्षित किया है क्योंकि यह बिना किसी समझौता के सतत विकास के लिए सबसे बड़ा और सबसे आशाजनक स्रोत है। पर्यावरण की गुणवत्ता के साथ। इलेक्ट्रोकेमिकल वाटर स्प्लिटिंग के माध्यम से हाइड्रोजन और ऑक्सीजन का उत्पादन विशेष रूप से लाइट असिस्टेड यानी फोटो-इलेक्ट्रोकेमिकल (पीईसी) वाटर स्प्लिटिंग रिएक्शन ऊर्जा के टिकाऊ और स्वच्छ स्रोतों की दिशा में एक आकर्षक समाधान है। आखिरकार, यह सौर ऊर्जा से संबंधित छिटपुट भंडारण समस्या का जवाब देने वाली प्रमुख तकनीकों में से एक बन गई है। थीसिस का उद्देश्य फोटोइलेक्ट्रोकेमिकल (पीईसी) जल विभाजन और हाइड्रोजन विकास प्रतिक्रिया उत्प्रेरक में आवेदन के लिए इन-सीटू हीटिंग और हाइड्रोथर्मल जैसे सरल तरीकों से विभिन्न नैनो और नैनोहेटरोस्ट्रक्चर सामग्री को संश्लेषित और चिह्नित करना है। इन दोनों क्षेत्रों में भविष्य की ऊर्जा मांगों को पूरा करने और वर्तमान ऊर्जा संकट परिदृश्य को हल करने की अपार संभावनाएं हैं। संक्रमण धातु आधारित उत्प्रेरक का अध्ययन अन्य धातुओं पर उनके कई लाभों के कारण किया जाता है, जैसे कि लागत प्रभावी विशेषताएं, इलेक्ट्रॉनिक संरचना का आसान संशोधन, आसान संश्लेषण, बहुमुखी गतिविधि और पीएच मान की विस्तृत श्रृंखला के तहत स्थिरता।

थीसिस मेटल ऑक्साइड नैनोस्ट्रक्चर और मेटल ऑक्साइड और ग्रेफाइटिक कार्बन नाइट्राइड ($g-C_3N_4$) के नैनोहेटरोस्ट्रक्चर से संबंधित है। ऑक्सीजन विकास प्रतिक्रिया के लिए फोटोइलेक्ट्रोकेटलिटिक गतिविधि और हाइड्रोजन विकास प्रतिक्रिया के लिए इलेक्ट्रो उत्प्रेरक की जांच की गई। इन-सीटू सॉलिड-स्टेट हीट ट्रीटमेंट का उपयोग करते हुए ग्रेफाइटिक-कार्बन नाइट्राइड ($g-C_3N_4$) के साथ निकल/निकल ऑक्साइड (Ni/NiO) हेक्सागोनल नैनोशीट के बीच 2D/2D इंटरफेस का संश्लेषण किया गया, जिसके परिणामस्वरूप उच्च विद्युत

रासायनिक और PEC जल विभाजन हुआ। 190 एमवी की अधिक क्षमता पर 20 एमए सेमी⁻² के अधिकतम ओईआर फोटोक्रेक्ट घनत्व को दर्शाने वाले 2डी/2डी इंटरफेस की गतिविधि। NiO के लिए पूर्ववर्ती प्रभाव के अनुपात को g-C₃N₄ अर्थात् g-C₃N₄ से भिन्न करना। 1:1, 1:8, और 1:16 का भी अध्ययन किया गया। जिनमें से, NiO से g-C₃N₄ नैनोशीट्स (यानी 1:1) का उच्चतम अनुपात इलेक्ट्रोकेमिकल (एचईआर) हाइड्रोजन विकास प्रतिक्रिया की दिशा में सबसे अच्छा प्रदर्शन प्रदर्शित करने के लिए नोट किया गया था, जो कि वर्तमान घनत्व को चलाने के लिए नाटकीय रूप से 26 mV से कम दिखा रहा है। ओईआर के लिए सेमी⁻² और 1:8। बढ़े हुए परिणाम जी-सी₃एन₄ के साथ एनआईओ की 2डी शीट के बीच अधिक घनिष्ठ संपर्क के कारण हो सकते हैं। नेक्स्ट निकेल इनकॉर्पोरेटेड ग्रेफाइटिक कार्बन नाइट्राइड समर्थित कॉपर सल्फाइड ने कुशल नोबल-मेटल-फ्री फोटो-इलेक्ट्रोकेमिकल वाटर स्प्लिटिंग के लिए सूचना दी। निकल-निगमित ग्रेफाइटिक कार्बन नाइट्राइड (Ni/g-C₃N₄@CuS) शीट्स पर समर्थित इन कॉपर सल्फाइड्स ने p-n जंक्शन के निर्माण के कारण PEC गतिविधि में सुधार किया। Ni/g-C₃N₄@CuS नैनोहाइब्रिड प्रकाश की रोशनी के तहत वर्तमान घनत्व में लगभग तीन गुना वृद्धि को दर्शाता है जो ca की अधिक क्षमता पर 15.5 mA सेमी⁻² तक पहुंचता है। अंधेरे की तुलना में 600 mV और इसकी मूल सामग्री, CuS और g-C₃N₄ की तुलना में लगभग पंद्रह गुना वृद्धि। आगे का काम हेक्सागोनल शीट्स और ट्यूबों के इन-सीटू सॉलिड-स्टेट सिंथेसिस कॉम्बिनेशन पर किया जाता है, जिसमें फोटो-इलेक्ट्रोकेमिकल वाटर स्प्लिटिंग को बढ़ाया जाता है। MoO₃ पर g-C₃N₄ शीट की संरचना का प्रभाव अर्थात् 1:1, 8:1, और 16:1 का अध्ययन किया गया है। इनमें से 8:1 (अर्थात् 8 भाग g-C₃N₄ और 1 भाग MoO₃) PEC गतिविधि के लिए सर्वश्रेष्ठ पाए गए हैं। उक्त हेटेरोजंक्शन से पीईसी गतिविधि में सुधार होता है, जिसमें 190 एमवी की अधिक क्षमता पर 4.96 एमए सेमी⁻² की फोटोक्रेक्ट घनत्व होता है। इसके बाद हमने दो धातु ऑक्साइड Ni/NiO और Co₃O₄ से बने टर्नरी नैनोहेटेरोस्ट्रक्चर का अध्ययन करने की कोशिश की, जिसमें ग्रेफाइटिक कार्बन नाइट्राइड 2D/3D इंटरफेस बनाते हैं। टर्नरी नैनोहेटेरोस्ट्रक्चर्स के

इस गठन से पीईसी प्रतिक्रिया में वृद्धि होती है, जी-सी₃एन₄/एनआईएनओ/सीओ₃ओ₄ को जी-सी₃एन₄/एनआईएनआईओ का 2.5 गुना और व्यक्तिगत कंपोजिट की तुलना में 5.8 गुना जी-सी₃एन₄/सीओ₃ओ₄ अधिक होने का उल्लेख किया गया था। इसके अलावा, एचईआर और ओईआर के लिए हेटेरोजंक्शन पर अध्ययन करते हुए हमने मेथनॉल ऑक्सीकरण और मेथनॉल सहायता प्राप्त विद्युत रासायनिक जल विभाजन के अध्ययन के लिए उत्प्रेरक विकसित करने का भी प्रयास किया। हमने डेंड्राइटिक हेमेटाइट की सतह पर एजी नैनोकणों को सजाने की कोशिश की। हमने अतिरिक्त मेथनॉल राशि में वृद्धि के साथ पानी के बंटवारे के लिए बढ़ी हुई इलेक्ट्रो उत्प्रेरक गतिविधि का अवलोकन किया, जिसे हेमेटाइट डेंड्राइट्स के सहक्रियात्मक प्रभाव के लिए जिम्मेदार ठहराया जा सकता है, डेंड्राइट संरचना का बड़ा सतह क्षेत्र एजी एनपी के उच्च लोडिंग के लिए अग्रणी है। विवरण में अध्यायों के बाद, थीसिस वर्तमान निष्कर्ष और भविष्य का दायरा है जहां हम धातु ऑक्साइड के साथ हेटरोस्ट्रक्चर बनाकर जी-सी₃एन₄ को संशोधित करने की योजना बनाते हैं और नई सामग्री का सुझाव देते हैं ताकि कुशल पीईसी परिणाम हो और इंटरफ़ेस पर चार्ज-ट्रांसफर प्रक्रिया को अनुकूलित किया जा सके।

TABLE OF CONTENTS

<i>CERTIFICATE</i>	<i>vi</i>
<i>ACKNOWLEDGEMENTS</i>	<i>viii</i>
<i>ABSTRACT</i>	<i>x</i>
<i>TABLE OF CONTENTS</i>	<i>xviii</i>
<i>LIST OF FIGURES</i>	<i>xxii</i>
<i>LIST OF TABLES</i>	<i>xxx</i>
<i>GLOSSARY OF SYMBOLS AND ABBREVIATIONS</i>	<i>xxxii</i>

CHAPTER 1

Introduction

<i>1.1 Introduction and Scope</i>	<i>1</i>
<i>1.2 Concept of Photoelectrochemical water splitting</i>	<i>2</i>
<i>1.3 Experimental Methodology</i>	<i>17</i>
<i>1.4 Strategies for Modifying Semiconductor for enhanced Photocurrent and Stability</i>	<i>22</i>
<i>1.5 Statement of Thesis Work</i>	<i>35</i>

CHAPTER 2

In-Situ solid-state synthesis of 2D/2D interface between Ni/NiO hexagonal nanosheets supported on g-C₃N₄ for enhanced photo-electrochemical water splitting

<i>2.1 Abstract</i>	<i>41</i>
<i>2.2 Introduction</i>	<i>41</i>
<i>2.3 Materials and Methods</i>	<i>43</i>

<i>2.4 Results and Discussion</i>	47
<i>2.5 Photoelectrochemical Measurements</i>	57
<i>2.6 Conclusion</i>	63
<i>2.7 References</i>	65

CHAPTER 3

Nickel Incorporated Graphitic Carbon Nitride Supported Copper Sulfide for Efficient Noble-Metal-Free Photo-electrochemical Water Splitting

<i>3.1 Abstract</i>	67
<i>3.2 Introduction</i>	68
<i>3.3 Materials and Methods</i>	71
<i>3.4 Results and Discussion</i>	75
<i>3.5 Conclusions</i>	96
<i>3.6 References</i>	97

Chapter 4

In-Situ solid-state synthesis combination of hexagonal sheets and tubes a composite of MoO₃ / g-C₃N₄ for enhanced photo-electrochemical water splitting

<i>4.1 Abstract</i>	101
<i>4.2 Introductio</i>	101
<i>4.3 Experimental Section</i>	103
<i>4.4 Results and Discussion</i>	105
<i>4.5 Conclusions</i>	120
<i>4.6 References</i>	120

Chapter 5

In-Situ solid-state synthesis of nano ternary heterostructure, a 2D/3D interface between Ni/NiO, Co₃O₄ hexagonal nanosheets supported on g-C₃N₄ for enhanced photo-electrochemical water splitting

5.1 Abstract.....	123
5.2 Introduction.....	124
5.3 Materials and Methods	126
5.4 Results and Discussions.....	128
5.5 Conclusions	141
5.6 References	142

Chapter 6

Multifunctional plasmonic Ag-hematite nano-dendrite electro-catalysts for methanol assisted water splitting: synergism between silver nanoparticles and hematite dendrites

6.1 Abstract.....	145
6.2 Introduction.....	145
6.3 Experimental Section	149
6.4 Results and Discussions.....	151
6.5 Conclusion.....	167
6.6 References	168

Chapter 7

<i>Summary and Future Prospects</i>	171
7.1 Summary.....	171
7.2 Future Scope	175

LIST OF FIGURES

<i>Figure</i>	<i>Figure Caption</i>	<i>Page</i>
<i>No.</i>		<i>No.</i>
<i>1.1</i>	<i>Basic configuration of PEC cell consisting of three electrodes and an electrolyte. The reactions at anode and cathode are also shown.</i>	<i>3</i>
<i>1.2</i>	<i>Steps involved in fabrication of working electrode for PEC water splitting.</i>	<i>3</i>
<i>1.3</i>	<i>Basic principle of PEC water splitting cell representing the generation of electron and hole in the presence of light.</i>	<i>4</i>
<i>1.4</i>	<i>Different types of photo electrochemical cells, (a) counter electrode with photo anode, (b) counter electrode with photo cathode and (c) both photo anode and photocathode without counter electrode.</i>	<i>5</i>
<i>1.5</i>	<i>Different types of heterojunctions with their band positions and water splitting charge transfer mechanisms.</i>	<i>6</i>
<i>1.6</i>	<i>Band gap values and band edge positions of some of the well-known semiconductors.</i>	<i>8</i>
<i>1.7</i>	<i>Ideal straddling condition of conduction and valence band edges of a semiconductor.</i>	<i>9</i>
<i>1.8</i>	<i>Representation of two complimentary reaction of water splitting into their respective constituents.</i>	<i>12</i>
<i>1.9</i>	<i>Representation of PEC water splitting mechanism using Photo anode as a photo electrode.</i>	<i>13</i>
<i>1.10</i>	<i>Representation of PEC water splitting mechanism using Photo cathode as a photo electrode.</i>	<i>13</i>

- 1.11** Energy band diagram for p-n junction presenting generation of photoelectrons and their movement. 14
- 1.12** (a) Sample dispersion ready for drop cast, (b) Fabricated working electrode for HER and (c) fabricated working electrode for PEC. 18
- 1.13** Pictorial representation of CV curve for a reversible electron transfer system 19
- 1.14** Schematic representing the donor and acceptor level due to the metal doping. 24
- 1.15** Band alignment and charge transfer mechanism of (A) type I, (B) type II, (C) type III, and (D) direct Z-scheme. VB is valence band; CB is conduction band; HER, hydrogen evolution reaction; OER, oxygen evolution reaction. 34
- 2.1** Powder XRD pattern of NiO, g-C₃N₄ nanosheets and their nanocomposites with varying compositional ratio viz. g-C₃N₄@NiO, g-C₃N₄@1/8NiO and g-C₃N₄@1/16NiO. 47
- 2.2** XPS core level spectra of g-C₃N₄ corresponding to (a) C 1s and (b) N 1s fitted with Shirley background using origin software. 48
- 2.3** XPS profile spectra of g-C₃N₄@NiO, nanocomposites corresponding to C1s {(a), (d), (g)}, Ni2p {(b), (e), (h)}, and O1s {(c), (f), (i)}. 50
- 2.4** TEM images of the as prepared nanocomposites with varying ratios of g-C₃N₄ and NiO (a-e), and SAED pattern (f) for g-C₃N₄@1/8NiO. 51

- 2.5 *Overlay of FTIR (a) and optical (b) spectra of the prepared nanocomposites with varying compositional ratio along with their parent materials.* 53
- 2.6 *(a) Current-potential plots showing HER performances and (b) EIS analysis.* 54
- 2.7 *Tafel plots (η vs. log current) for HER currents.* 56
- 2.8 *(a) Current-potential curves recorded on NiO, g-C₃N₄ and their composites under dark and light irradiation showing PEC performances of the composite sample (b) EIS analysis of these materials at an over potential of 140 mV.* 58
- 2.9 *Tafel plots (η vs. log current) for OER drawn from linear sweep polarization curves for composites.* 60
- 2.10 *Mott-Schottky plots for the nanocomposites obtained with varying composition. The response from bare NiO and g-C₃N₄ is also overlaid.* 61
- 2.11 *(a), plots of Histogram representing the corresponding Debye lengths. (b) Plots of space charge layer width against the applied potential for the samples.* 63
- 3.1 *Powder XRD pattern of CuS, g-C₃N₄, Ni/g-C₃N₄ and Ni/g-C₃N₄@CuS samples. The bar diagram for JCPDS file numbers 87-0712, and 75-2233 are also plotted for comparison.* 77
- 3.2 *XPS core-level spectra corresponding to C 1s and N 1s for g-C₃N₄ [(a) and (b)] and Ni/ g-C₃N₄@CuS [(c) and (d)] fitted with Shirley background using origin software.* 79

3.3	<i>XPS core level spectra of Ni/g-C₃N₄ and Ni/g-C₃N₄@CuS corresponding to Ni 2p {(a), (b)}, Cu 2p (c) and S 2p (d).</i>	80
3.4	<i>UV-vis diffuse reflectance spectra (UV-vis DRS).</i>	82
3.5	<i>Plot of $(ah\nu)^2$ vs. photon energy ($h\nu$), of (a) g-C₃N₄, (b) Ni/g-C₃N₄ (c) Ni/g-C₃N₄@CuS and (d) CuS.</i>	83
3.6	<i>SEM images of the as-prepared nanocomposites (a) g-C₃N₄ (b) Ni/g-C₃N₄(c) CuS (d) Ni/g-C₃N₄@CuS.</i>	84
3.7	<i>TEM images of the as-prepared nanocomposites (a) g-C₃N₄ (b) Ni/g-C₃N₄ (c) CuS (d) Ni/g-C₃N₄@CuS.</i>	85
3.8	<i>(a) Current-potential curves at showing PEC performances and (b) EIS analysis of the composite materials. An inset shows zoomed portion of the Nyquist plots for Ni/g-C₃N₄ and Ni/g-C₃N₄@CuS.</i>	86
3.9	<i>(a) Tafel plots (η vs. log current) for OER currents (b) Transient photocurrent density versus time curves for the synthesized samples.</i>	89
3.10	<i>Mott-Schottky plots for the nanocomposites (a) overlaid of three samples (b) CuS.</i>	91
3.11	<i>The graph depicting variation in Width of depletion layer as a function of applied potential for different samples.</i>	94
4.1	<i>Powder XRD pattern of MoO₃, g-C₃N₄ nanosheets, and the nanocomposites with MoO₃ with varying compositional ratio viz. g-C₃N₄@MoO₃, 8g-C₃N₄@1MoO₃, and 16g-C₃N₄@1MoO₃.</i>	107
4.2	<i>Overlay of FTIR spectra for different samples utilized for the present study.</i>	107

4.3	<i>Plot of $(ah\nu)^2$ vs. photon energy $(h\nu)$, of g-C₃N₄, MoO₃, and nanocomposites.</i>	108
4.4	<i>Raman spectra of MoO₃ and nanocomposites at room temperature.</i>	109
4.5	<i>XPS core-level spectra corresponding to C 1s for g-C₃N₄ and composite materials</i>	110
4.6	<i>XPS core-level spectra corresponding to N 1s for g-C₃N₄ and composite materials.</i>	111
4.7	<i>XPS profile spectra of MoO₃, corresponding to Mo 3d and O 1s.</i>	112
4.8	<i>XPS profile spectra of g-C₃N₄@MoO₃, corresponding to Mo 3d and O 1s.</i>	113
4.9	<i>SEM images of the as-prepared nanocomposite</i>	114
4.10	<i>TEM images of the as-prepared nanocomposites.</i>	115
4.11	<i>(a) Current-potential curves recorded at showing PEC performances and (b) Zoomed portion of LSV.</i>	116
4.12	<i>(a) EIS analysis of nanocomposites and parent materials. (b) Tafel plots (η vs. log current) for OER currents in light.</i>	117
4.13	<i>Mott Schottky plots for g-C₃N₄, MoO₃, and their nanocomposites.</i>	118
4.14	<i>Transient photocurrent density versus time curves for the synthesized samples.</i>	119
5.1	<i>Powder XRD pattern of g-C₃N₄ Nanosheets and the nanocomposites viz. g-C₃N₄/NiNiO, g-C₃N₄/Co₃O₄, and g-C₃N₄/NiNiO/Co₃O₄.</i>	130

5.2	<i>Overlay of FTIR spectra (a) and optical spectra (b) for different nanocomposite samples.</i>	130
5.3	<i>EDX spectra of the g-C₃N₄, and its variant nanocomposites.</i>	131
5.4	<i>XPS core-level spectra of g-C₃N₄ corresponding to (a) C 1s and (b) N 1s fitted with Shirley background using origin software.</i>	132
5.5	<i>XPS core-level spectra of C 1s corresponding to g-C₃N₄/NiNiO (a), g-C₃N₄/Co₃O₄ (b), g-C₃N₄/NiNiO/Co₃O₄ (c), fitted with Shirley background using origin software.</i>	133
5.6	<i>XPS core-level spectra of Ni 2p corresponding to g-C₃N₄/NiNiO (a), g-C₃N₄/NiNiO/Co₃O₄ (b), fitted with Shirley background using origin software.</i>	134
5.7	<i>XPS core-level spectra of Co 2p corresponding to g-C₃N₄/NiNiO/Co₃O₄, g-C₃N₄/Co₃O₄ fitted with Shirley background using origin software.</i>	134
5.8	<i>TEM images of the as-prepared nanocomposites (a-d), and SAED pattern (e) for g-C₃N₄/NiNiO/Co₃O₄.</i>	136
5.9	<i>(a) Current-potential curves recorded for showing PEC performances of the composite sample (b) zoomed portion of the LSV.</i>	137
5.10	<i>(a) EIS analysis of the studied materials (b) Zoomed portion for better observation.</i>	138
5.11	<i>(a) Tafel plots (η vs. log current) for OER currents (b) Transient photocurrent density versus time curves for the synthesized samples.</i>	139

- 5.12** *Mott-Schottky plots for the (a) g-C₃N₄ (b) overlaid three 140 nanocomposites.*
- 6.1** *The UV-Vis spectra of hematite (black solid curve) and silver hematite 152 prepared by chemical co-precipitation method (red dotted curve) and hydrothermal treatment (blue dashed curve).*
- 6.2** *An overlay of XRD pattern for hematite dendrites along with Ag 154 decorated hematite dendrites prepared by hydrothermal and chemical treatment.*
- 6.3** *FESEM images of (a) Hematite (b) chemically prepared Ag-Hem (c) 156 hydrothermally prepared Ag-Hem. (d - f) elemental mapping of chemically prepared silver hematite catalyst showing the distribution of Fe, O and Ag.*
- 6.4** *TEM images and EDAX spectra of hematite (a and d), hydrothermally 157 prepared silver hematite (b and e) and chemically prepared silver hematite (c and f).*
- 6.5** *Electrochemical hydrogen evolution at different concentration of 160 methanol by (a) hematite (b) chemically prepared silver hematite (c) Hydrothermally prepared silver hematite and (d) silver NPs. An overlay*
- 6.6** *of CV curves recorded for Cp electrode modified with various 162 electrocatalysts in 0.5 M H₂SO₄ solution after addition of 800 μL of methanol. The scan rate was 50 mV/s. The response from Ag NPs is also overlaid for the comparisonn*

6.7	<i>Tafel plots for the HER polarization curves recorded on the electrocatalyst modified Cp electrodes.</i>	163
6.8	<i>Electrochemical OER in term of current-potential curves for hematite dendrites, AgHem and HyAgHem in 0.1 M KOH electrolyte solution.</i>	165
6.9	<i>(Left panel) Cyclic voltammograms in 0.5M H₂SO₄ for AgHem prepared by chemical co-precipitation method with successive addition of methanol, (Right panel) magnified view of selected area of the figure shown in left panel.</i>	166
6.10	<i>Electrochemical stability of the chemically prepared silver hematite for (a) hydrogen evolution reaction and (b) methanol oxidation reaction.</i>	166
6.11	<i>Photo corrosion study of chemically prepared silver hematite.</i>	167
7.1	<i>Schematic representation of ternary p-n heterojunction.</i>	176

Table No.	Table Caption	Page No.
1.1	<i>Comparison of the installed capital cost, production cost for different hydrogen production technologies.</i>	11
1.2	<i>Table showing the comparison of various dopants with achieved current density value in a particular electrolyte using AM 1.5 light source and a potential of 1.23 V vs.RHE.</i>	25
1.3	<i>Table showing the comparison of nanostructure catalyst with achieved current density value in a particular electrolyte using AM 1.5 light source at a given applied potential.</i>	26
1.4	<i>Table showing the comparison of nanostructure catalyst with achieved current density value with different synthesis method. The current density is measured at 1.23 V vs. RHE.</i>	27
1.5	<i>Table showing the comparison of surface passivation layer with achieved current density value, onset values and with different synthesis ways.</i>	28
1.6	<i>Table showing the summary of Quantum dot sensitization with photocurrent densities.</i>	31
2.1	<i>The HER electrodicts parameters obtained for all the electrocatalyst used in the present study.</i>	56
2.2	<i>Exchange current density and Tafel slope analysis for OER.</i>	61
3.1	<i>The physico-chemical characterization parameters along with kinetic parameters viz. Exchange current density and Tafel slope analysis from OER.</i>	90

6.1	<i>Elemental composition of HDs, HyAgHem and AgHem nanodendrite structures.</i>	158
6.2	<i>HER onset potential along with overpotential values required for 10 mA/cm² current density for different electro-catalysts modified Cp electrode at an addition of 800 μL of methanol.</i>	163

LIST OF ABBREVIATIONS AND SYMBOLS

EF	Fermi level (in V)
E _g	Bandgap energy (in eV)
JCPDS	Joint committee on powder diffraction standards
ε ₀	Permittivity of free space (= 8.85419x 10 ⁻¹² F m ⁻¹)
ε	Dielectric constant
EIS	Electrochemical impedance spectroscopy
EDX	Energy Dispersive X-Ray
FESEM	Field emission scanning electron microscopy
FT-IR	Fourier transformed infrared
FTO	Fluorine-doped tin oxide
ITO	Indium-doped tin oxide
LSV	Linear sweep voltammetry
CV	Cyclic Voltammetry
λ	Wavelength (in nm)
MS	Mott–Schottky
NHE	Normal Hydrogen Electrode
N _d	Donor density
PL	Photoluminescence
Pt	Platinum
Ag	Silver

PEC	Photo electrochemical
SPR	Surface plasmon resonance
SEM	Scanning electron microscopy
TEM	Transmission Electron Microscopy
XPS	X-ray Photoelectron Spectroscopy
FTIR	Fortier Transformed Infra-red spectroscopy
EIS	Electrochemical Impedance Spectroscopy
HER	Hydrogen Evolution Reaction
OER	Oxygen Evolution Reaction
W	Width of depletion layer
TEM	Transmission electron microscopy
UV-VIS	Ultraviolet visible
XRD	X-ray diffraction
XPS	X-ray photo spectroscopy
CP	Carbon paper
EDX	Elemental Dispersive X-ray Spectra
GCE	Glassy carbon electrode
g-C ₃ N ₄	Graphitic carbon nitride
L _D	Debye length
J _o	Exchange Current
T	Temperature (in K or °C)